THE JOURNAL OF CHEMICAL PHYSICS **123**, 134902 (2005)

Molecular dissipation phenomena of nanoscopic friction in the heterogeneous relaxation regime of a glass former

Scott Sills, Tomoko Gray, and René M. Overney[a)]
Department of Chemical Engineering, University of Washington,
Seattle, Washington 98195-1750

(Received 8 June 2005; accepted 27 July 2005; published online 3 October 2005)

Nanoscale sliding friction involving a polystyrene melt near its glass transition temperature T_g (373 K) exhibited dissipation phenomena that provide insight into the underlying molecular relaxation processes. A *dissipative* length scale that shows significant parallelism with the size of cooperatively rearranging regions (CRRs) could be experimentally deduced from friction-velocity isotherms, combined with dielectric loss analysis. Upon cooling to ~10 K above T_g, the dissipation length X_d grew from a segmental scale of ~3 Å to 2.1 nm, following a power-law relationship with the reduced temperature $X_d \sim T_R^{-\phi}$. The resulting $\phi=1.89\pm0.08$ is consistent with growth predictions for the length scale of CRRs in the heterogeneous regime of fragile glass formers. Deviations from the power-law behavior closer to T_g suggest that long-range processes, e.g., the normal mode or ultraslow *Fischer* modes, may couple with the α relaxation, leading to energy dissipation in domains of tens of nanometers. © *2005 American Institute of Physics*.

[DOI: 10.1063/1.2038907]

I. INTRODUCTION

A nanoscopic description of polymer dynamics involves, in general, only two parameters: an internal, or monomeric, friction coefficient and an appropriate macromolecular length scale.[1] Monomeric friction dictates the degree of local segmental motion and thus is responsible for the bulk viscoelastic and relaxational properties of polymeric materials. Since Grosch[2] and Ludema and Tabor,[3] a molecular length scale for bulk viscoelasticity has been accessible in friction experiments involving *elastomers* in sliding contact with *hard* surfaces. The friction force was found to vary with temperature and velocity according to the Williams, Landel, and Ferry (WLF) superposition principle.[4] Friction-velocity $F_F(v)$ isotherms showed distinct peaks at a critical velocity, which if combined with characteristic viscoelastic frequencies provide critical lengths on the order of 5–10 nm.[2,3] Segmental chain slippage was suspected as the basic mechanism for sliding dissipation.[2,3] Early interpretations by Schallamach[5] and Ludema and Tabor[3] addressed the friction-related segmental motions of the polymer chain from two different viewpoints: Schallamach considered the friction force in terms of a fully adhesive, rate-dependent molecular debonding model, introduced by Kantorova and Frenkel[6] and Eyring[7] and later improved by Chernyak and Leonov.[8] Ludema and Tabor, on the other hand, suggested an adhesive viscoelastic model in which the energy dissipated during sliding is lost in the deformation of the soft material. In recent work involving *smooth* macroscopic contacts, the importance of both processes during steady sliding was recognized.[9] In this article, we address the issue of bulk viscoelastic friction from a nanoscopic perspective. Our results provide molecular insight into the dissipation process in amorphous polystyrene, a material technologically relevant to photonics,[10,11] electronics,[12] and nanoelectromechanical systems (NEMS).[13] We show that both the energetics involved in frictional dissipation and the length scale over which the energy is dissipated can be linked to the molecular relaxation processes that evolve during the glass transition.

II. EXPERIMENT

The nanoscopic thermorheological behavior of atactic polystyrene (PS) (M_w=96.5 kg/mol, M_w/M_n=1.04; Polymer Source, Inc.) was investigated in the glass-forming region above the glass transition temperature with friction force microscopy (FFM).[14,15] Polystyrene was spin cast from a cyclohexanone (Mallinckrodt Baker, Inc.) solution onto silicon. The 156±8-nm-thick film was annealed at 160 °C for 4 h under vacuum. A glass transition temperature T_g of 373±1 K was determined with shear-modulated force microscopy (SM-FM) (Ref. 16) and found to be consistent with the bulk value of PS.

FFM measurements were conducted under N_2 (5±2 % relative humidity) using a bar-shaped silicon cantilever (Nanosensors) with a normal spring constant k_N =0.164 N/m and a lateral spring constant k_T of approximately 80 N/m. Friction forces were determined from the hysteresis in the torsional cantilever deflection between forward and reverse scans[14,17] and were calibrated following the procedure of Buenviaje *et al.*[17] Scanning was performed over a 0.5–10 μm range with a 20 nm line spacing to avoid overlapping scan lines. No single line was scanned more than once, to minimize any memory effects associated with successive scanning of the same location. This procedure minimizes compound effects associated with large-scale, shear-induced surface deformations such as bundle formation,[18]

[a)] Author to whom correspondence should be addressed. Electronic mail: roverney@u.washington.edu

© 2005 American Institute of Physics

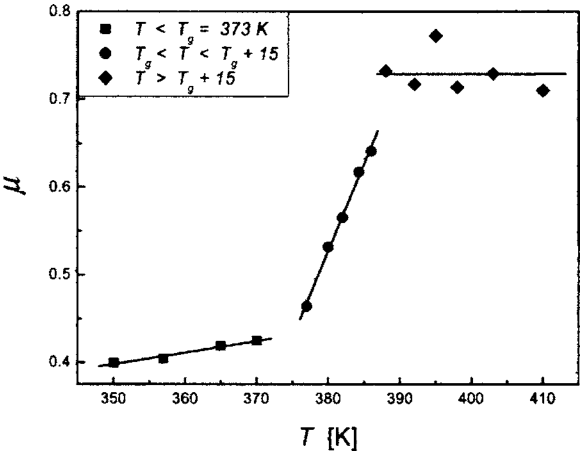

FIG. 1. Friction coefficient (μ) of PS. Below T_g of 373 K, the friction coefficient reflects dissipation in the glass. Within 15 K above T_g, the friction coefficient undergoes a continuous transition from the glass to the fully developed melt above T_g+15 K.

and avoids artificially altering the potential barrier heights related to the material's intrinsic relaxation properties.

Isothermal friction-velocity curves were recorded over a velocity range of five decades, from 10 to 10^5 nm/s for temperatures between 377 and 420 K. The friction-rate data are reported for a constant applied load of zero nanonewton under an average adhesive load of 91 nN. The friction-rate isotherms reveal a temperature-dependent critical velocity $v_o(T)$ corresponding to a maximum in the friction force (see results and discussion). In a separate experiment, the friction coefficient $\mu(T)$ was measured over a temperature range of 350–410 K at a scanning velocity corresponding to $v_o(T)$ for $T > T_g$ and $v = 2.0$ μm/s for $T < T_g$, where no critical velocity is observed in the accessible range.[19] The friction coefficient represents the friction force normalized by the normal load (the sum of the applied and adhesive loads) which ranged from 3 to 182 nN. Thus, for non-negative applied loads, the behavior of $\mu(T)$ accounts for any load-dependent changes in the contact area.

III. RESULTS AND DISCUSSION

A first glance of the frictional behavior on polystyrene near its glass transition is illustrated with the temperature-resolved friction coefficient $\mu(T)$ in Fig. 1. The friction coefficient reveals three regimes: (i) a single glassy phase below T_g; (ii) a transitional regime within 15 K above T_g; and (iii) a *fully developed* melt above 388 K. In the glassy phase, a friction coefficient of 0.40–0.43 agrees with the room-temperature value of 0.39 reported for FFM measurements on monodisperse PS of comparable molecular weight.[20] Furthermore, the glassy friction coefficient also agrees with the macroscopic values of 0.40–0.51.[21,22] The transition in the friction coefficient from the glass to the melt is not abrupt, but ranges over 15 K starting at T_g. During the transition, the friction coefficient increases by 0.023 per unit Kelvin to a value of 0.73 in the fully developed melt, which is consistent with a 0.744 value for the bulk PS melt.[22]

To illuminate the molecular mechanisms responsible for the frictional behavior in Fig. 1, we evaluated the amount of energy that the material dissipates during frictional sliding. Based on earlier work involving only glassy PS,[19] we determined the potential barrier that is continuously overcome during sliding of the FFM tip by time-temperature superposition of friction-velocity isotherms using *the method of reduced variables*.[23] Under this formalism, one obtains a thermal shift factor a_T by laterally shifting the $F_F(v)$ isotherms with respect to a reference temperature (420 K), as illustrated in Fig. 2(a). Superposed friction-velocity isotherms for PS above the glass transition are reported in Fig. 2(b), revealing nanoscopic features similar to observations in macroscopic sliding experiments on polymers.[2,3] An activation barrier of 81 kcal/mol (3.5 eV) is deduced from the *apparent* Arrhenius behavior of a_T in the inset Fig. 2(b). The value coincides with the 80–90 kcal/mol activation energy for the α-relaxation process.[24] Thus, frictional dissipation above T_g is dominated by the α relaxation, i.e., the segmental relaxation of the PS backbone, and its value exceeds, by one order of magnitude, the 7 kcal/mol dissipation barrier for phenyl side-chain rotations below T_g, previously determined by FFM.[19] Similarly, the interplay of frictional dissipation and molecular side-chain relaxation has been shown in glassy poly(methyl methacrylate).[25]

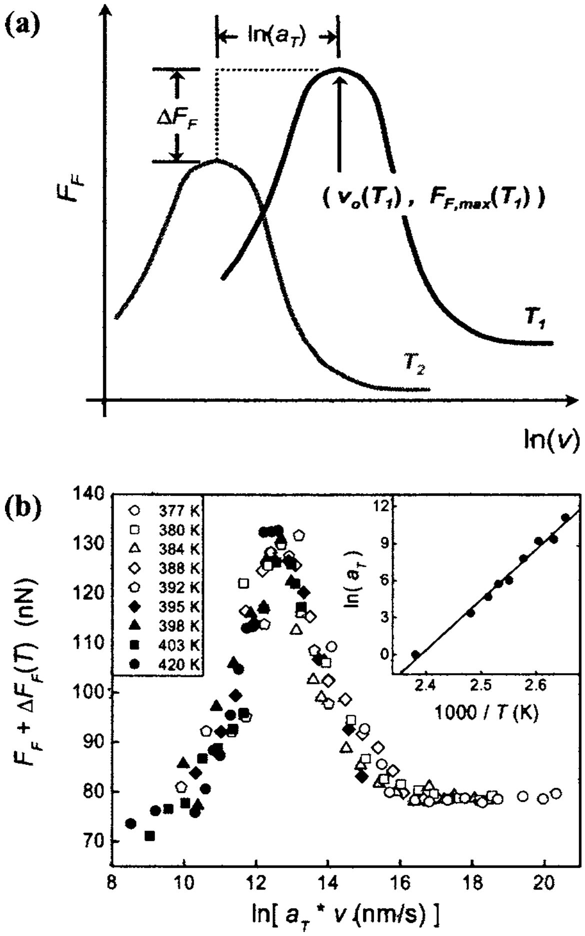

FIG. 2. Friction force-velocity, $F_F(v)$, isotherms. (a) Generic $F_F(v)$ isotherms with temperatures $T_1 > T_2$. The maximum friction intensity $F_{F,\max}$ at v_o serves as the reference point for superposition. (b) $F_F(v)$ isotherms for polystyrene above T_g=373 K, superposed using the method of reduced variables and a reference temperature of 420 K. Inset: From the Arrhenius behavior of a_T, an average activation energy E_A of 81 kcal/mol identifies the α relaxation as responsible for frictional dissipation.

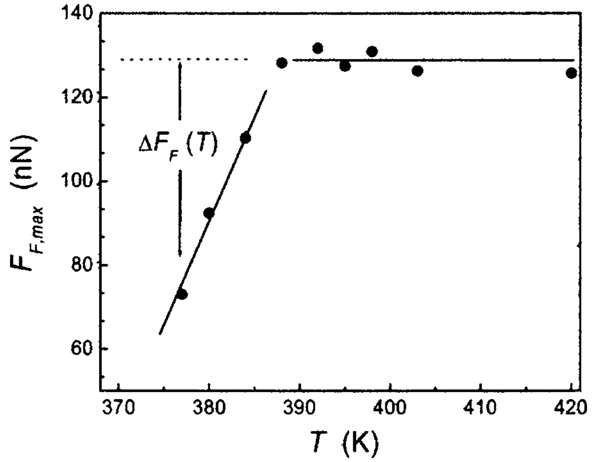

FIG. 3. Friction-peak intensity $F_{F,\max}(T)$ for the α relaxation, $\Delta F_F(T) = F_{F,\max}(T > T_g + 15) - F_{F,\max}(T)$. A constant peak intensity for $T > 388$ K indicates a structurally homogeneous melt. Attenuation of the peak intensity as T_g is approached ($T_g < T < T_g + 15$ K) reveals the heterogeneous nature of the glass transition and suggests dissipation through lower-energy side-chain relaxations.

While the thermal shift of friction-velocity isotherms provides an energetic signature for the dissipation mechanism, at least two intrinsic properties of that mechanism are reflected in the bell-shaped $F_F(v)$ isotherms of Fig. 2(b). Ludema and Tabor[3] explained the $F_F(v)$ peak with respect to the variation of the contact area and the shear strength with scan velocity. Thus, friction expressed as $F_F(a_T v) = \sigma(a_T v) A(E(v))$ will exhibit a bell-shaped curve similar to Fig. 2(b), where σ represents the shear stress, A the real contact area, and $E(v)$ the viscoelastic modulus. The qualitative rate behavior of both the shear strength and modulus, and thus the shape of the $F_F(v)$ curve, originates from the interplay of two dominating time scales: (i) the extrinsic drive time τ_e dictated by the sliding velocity v and (ii) the intrinsic material response time τ_m which in this case is the α-relaxation time τ_a. The friction force increases or decreases with increasing sliding velocity depending on whether the extrinsic time leads or trails the material response time, respectively. In the vicinity of the $F_F(v)$ peak, the two processes occur on comparable time scales. Hence, the maximum friction force $F_{F,\max}(T)$ and the velocity $v_o(T)$ corresponding to $F_{F,\max}(T)$ are characteristic of the α relaxation.

The *α-friction-peak* intensity, $F_{F,\max}(T)$ in Fig. 3, was obtained from $F_F(v)$ data prior to the superposition in Fig. 2. The friction-peak intensity behaves similar to the friction coefficient in Fig. 1, with a distinct phase separating temperature at 388 K. The temperature-independent friction-peak intensity above 388 K indicates a fully developed melt. Below 388 K, the friction-peak intensity diminishes on cooling toward T_g, which identifies the vertical shift $\Delta F_F(T)$ depicted and utilized in Figs. 1(a) and 1(b), respectively. From the Arrhenius behavior of a_T in Fig. 2(b), the energy per dissipation event may be considered constant, thus the 4.9-nN/K attenuation of the α peak in the transition regime indicates that the number of α-dissipation events decreases. This behavior suggests a heterogeneity of two structural phases. Based on the continuity of the friction coefficient across the transition region in Fig. 1, the heterogeneity reflects a spatial distribution of dissipation through independent backbone and side-chain relaxations. In a simple picture, small domains or threads of the glass phase begin to appear near 388 K, diluting the α-peak intensity with lower-energy dissipation through phenyl side chains. As the temperature decreases, the remaining melt phase becomes consumed by the glass and the α-peak intensity diminishes.

The observation of a temperature range for the glass transition, as opposed to a singularity at the calorimetric T_g, is not unique to FFM. Internal friction dictates the relaxational and diffusive behaviors of polymers through the modified Rouse theory and the Stokes-Einstein law, respectively. Hence, it is not surprising that a similar transitional region is found in both dielectric relaxation[26,27] and translational and rotational diffusion measurements (Ref. 28 and references therein). In fact, experimental evidence indicates that many glass formers exhibit distinct changes within a narrow and well-defined time-temperature range, referred to as the *crossover region* of the dynamic glass transition.[27] Within the crossover region, the translational diffusion decouples from the Stokes-Einstein relationship. The crossover is also discussed based on a bifurcation of a single primary relaxation mode at higher temperatures, into both *slow* (α) and *fast* (β) relaxation processes in the crossover regime.[29] While the slow α relaxation becomes frozen at T_g, the fast process, identified in PS as the local rotation of the phenyl-ring side chains,[30] continues below T_g and actively contributes to frictional dissipation in the glass phase.[19] Unfortunately, the frequency (i.e., velocity) bandwidth of the FFM is not sufficient to capture the fast rotational peak in the melt phase, which we expect at a velocity on the order of centimeters per second. The high-temperature limit of the glass transition is the crossover temperature T_c, which marks the breakdown of the Rouse-type behavior due to dynamical heterogenieties.[26] T_c is generally found several tens of degrees above T_g.

Discussing the dynamics of the glass-forming process with respect to the crossover temperature is one school of thought. Another approach is to express data in the light of a critical low-temperature limit based on thermodynamic equilibrium arguments, which theoretically is the Kauzmann temperature, $T_k < T_g$, where the system entropy would become negative (Kauzmann paradox). The empirical analog to the Kauzmann temperature is the Vogel-Fulcher temperature T_o which is experimentally extrapolated to about 50 °C below T_g for many glass-forming polymers. In our experiment, the lower-temperature limit of the dynamic regime is identified by the extrapolated temperature $T_1 = 362$ K at which the α-peak intensity in Fig. 3 vanishes, i.e., $F_{F,\max}(T_1) = 0$.

For the ensuing discussion, we will employ the two critical temperatures deduced from our FFM analysis, $T_1 = 362$ K and $T_2 = 388$ K, in analogy to the Vogel-Fulcher and the crossover temperatures (T_o and T_c), respectively. Although the dynamic range defined by T_1 and T_2 is significantly narrower than the one defined by their counterparts T_o and T_c, we point out a rather unexpected correspondence of various dynamical quantities, such as the length scale of cooperativity, with state-of-the art classical experiments.

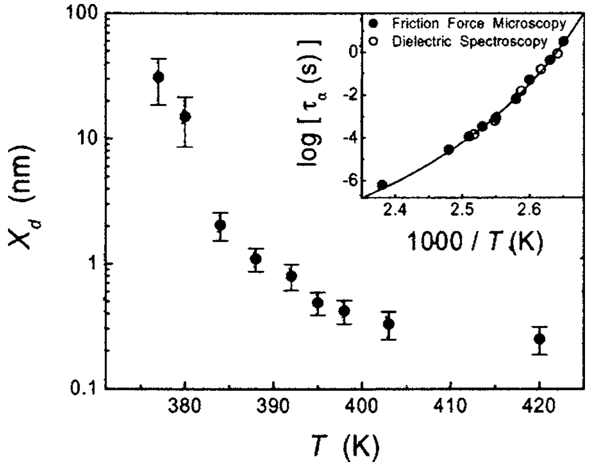

FIG. 4. The characteristic dissipation length scale X_d during the α relaxation of polystyrene near the glass transition ($T_g=373$ K). Error bars represent the experimental uncertainty in the velocity corresponding to the friction peak. Inset: Corresponding polystyrene α-relaxation times τ_α determined from the FFM friction peaks and Eq. (1) (closed circles) compared to dielectric spectroscopy measurements (Ref. 31) (open circles). The solid line represents a fit of the Vogel-Tamman-Fulcher equation: $\tau_\alpha=\tau_o \exp(B/(T-T_o))$ ($\tau_o=2.06e^{-12}$ s, $B=1019$ K, $T_o=341$ K).

The characteristic length of the dissipation process is deduced from the velocity corresponding to the friction peak $v_o(T)$ in Fig. 2(b). Similar to Grosch[2] and Ludema and Tabor,[3] who combined the velocity at the friction peak with the frequency for the maximum viscoelastic loss to deduce a dissipative length scale, we relate our friction-velocity results to dielectric spectroscopy data[31] for PS of comparable molecular weight ($M_w=90.0$ kg/mol, $M_w/M_n=1.06$). It is well founded that interpretations of dielectric relaxations relate directly to the time scale for mechanical relaxation.[32] Thus, with the specific knowledge of the α-relaxation times $\tau_\alpha(T)$ from the dielectric data and the critical velocities $v_o(T)$ corresponding to the friction peaks, the length scale over which energy is dissipated during an α-relaxation event may be expressed as

$$X_d(T)=v_o(T)\tau_\alpha(T). \tag{1}$$

The dissipation lengths associated with the α relaxation, $X_d(T)$, are presented semilogarithmically in Fig. 4. At first glance, the dissipation length appears to be distributed between two asymptotes: (i) a lower limit of ~0.3 nm in the fully developed melt ($T>400$ K), corresponding to relaxation at the segmental scale and (ii) a divergent $X_d(T)$ as T_g is approached, corresponding to complete vitrification. Technically, the low limit is below the monomer size; however, adequate resolution of this high-temperature limit requires a higher velocity bandwidth for FFM.

At this point, let us consider how the dissipation length is related to characteristic material dimensions. Relaxation processes in polymers are controlled by very different length scales, ranging from localized segmental relaxations covering only a few repeating units to long-range modes involving the whole polymer chain (the so-called normal mode).[26] While the length scale of the normal mode is related to fluctuations of the end-to-end vector of the polymer chain, the length scale for segmental motion during the α relaxation ξ_α is generally discussed in content of cooperatively rearranging regions (CRRs), or regions in space where the motion of an individual chain segment is contingent upon the orchestrated motion of an ensemble of N_α surrounding segments, with $N_\alpha \sim \xi_\alpha^3$ (Ref. 33). The length scale for cooperative motion during the α relaxation is predicted to be on the nanometer scale, involving ~100 monomer segments.[28,33–35] Estimates of ξ_α for many uncross-linked polymers, including polystyrene, range from 1 to 4 nm at T_g.[36,37] For polymers, direct observations of ξ_α are sparse (noted exception of Ref. 38) and direct experimental evidence for the temperature dependence of ξ_α is lacking,[34] which makes for a difficult comparison with $X_d(T)$.

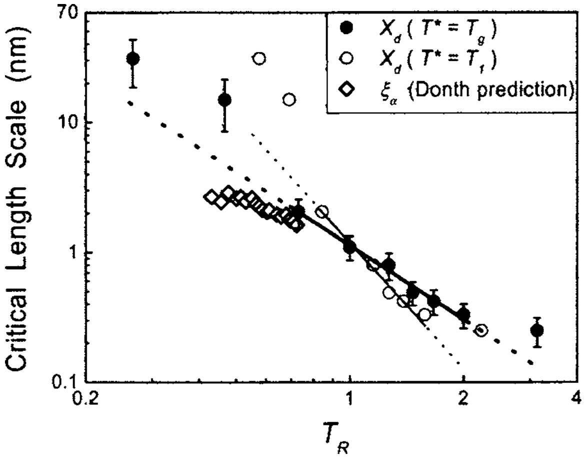

FIG. 5. Power-law representation of the FFM dissipation lengths X_d in terms of the reduced temperature T_R, i.e., $X_d \sim T_R^{-\phi}$. The closed circles represent the dissipation lengths with respect to $T_R(T^*=T_g)$. The power-law fit over the range of $0.7<T_R<2.0$ (thick solid line) reveals an exponent of $\phi=1.89\pm0.08$. The open circles represent the dissipation lengths with respect to $T_R(T^*=T_1)$. The power-law fit over the corresponding T_R range (thin solid line) reveals an exponent of $\phi=3.25\pm0.17$. The diamonds represent PS cooperation lengths ξ_α predicted by Donth (Ref. 36) and Huth (Ref. 43) ($\phi=1.5\pm0.10$). X_d error bars are omitted on the open circles for clarity and the dotted lines are extrapolations to the divergent points. Note that the nonreduced temperatures for $\xi_\alpha(T)$ from Ref. 43 ranged from 374–405 K.

The underlying question is whether the friction energy dissipated into the α relaxation is contained within CRRs ($X_d=\xi_\alpha$) or can it be transmitted across CRR domain boundaries ($X_d>\xi_\alpha$), effectively coupling to longer-range modes, e.g., the normal mode[26] or Fischer modes.[39] We have established above that the FFM probe is sensitive predominately to the α relaxation. Thus, given that the rearrangements within a CRR are connected with an average velocity $v_\alpha=\xi_\alpha/\tau_\alpha$ (Ref. 33), it is reasonable to discuss the α peak in Fig. 2(b) in conjunction with CRR rearrangements; i.e., assuming the experimental scan velocity of the α peak $v_o(T)$ matches the velocity of the CRR rearrangements $v_\alpha(T)$, Eq. (1) leads to $X_d(T)=\xi_\alpha(T)$.

For comparison with other work involving CRR dynamics, the X_d values from Fig. 4 are presented double logarithmically with the reduced temperature in Fig. 5, where the reduced temperature captures both the upper and lower critical temperatures for the range of the dynamic glass transition, i.e., $T_R=(T-T^*)/(T_2-T^*)$. One difficulty with reduced temperature plots is that they strongly depend on the low-temperature limit T^*. In our experiment, the observed low-temperature limit is T_g, while the extrapolated analog to the Vogel temperature is T_1. The dissipation lengths are reported for both interpretations of the low-temperature limit in Fig. 5. In both cases, for $T_R > 1$, the dissipation length falls below 1 nm, which is consistent with estimates for the characteristic relaxation length above the crossover regime $(T_R > 1)$.[27,40] The FFM data do not reveal any abrupt changes in the dissipation behavior at a critical length of ~ 1 nm that would support interpretations based on *minimal cooperativity*.[41]

When cooling from 403 to 384 K, the dissipation length increases steadily from 0.3 to 2.1 nm, following a power-law relation of the form $X_d \sim T_R^{-\phi}$ in Fig. 5. The power-law exponent ϕ is 3.25 ± 0.17 for $T_R(T^* = T_1)$ and 1.89 ± 0.08 for $T_R(T^* = T_g)$. The latter is consistent with predictions based on molecular-dynamics (MD) simulations $(\phi = 1.87 \pm 0.15)$ for the spatial correlation of segmental displacements above the critical temperature of the mode coupling theory $(T_R > 1)$.[42] Also apparent in Fig. 5, the dissipation lengths have a similar size and temperature dependence as the PS cooperation lengths ξ_α predicted by Donth[36] and Huth[43] $(\phi = 1.5 \pm 0.10)$. The ξ_α values represent the effective diameters of estimated CRR volumes V_α based on dynamic calorimetry and the Von Laue approach,[36,43] assuming a spherical geometry, i.e., $\xi_\alpha = 2[3V_\alpha/(4\pi)]^{1/3}$. The dissipation lengths are slightly higher than the ξ_α estimates by about 0.1 logarithmic decades. Typically, CRRs have a size distribution, which is limited at the lower end by the minimum size necessary for relaxation. This minimum size is closely linked to the configurational entropy of the system, from which thermodynamic and dynamic properties can be determined. The FFM dissipation lengths would represent a statistical mean of a CRR size distribution and hence could be expected to be greater than the minimum CRR size predicted theoretically.

On closer approach to $T_g (T < 384$ K), we find a strong deviation from the above power-law behavior, with dissipative domains of up to 31 nm. A single power-law fit through all points is mathematically possible if T^* is arbitrarily shifted to 376 K, which exceeds T_g and is physically unrealistic. Furthermore, the large dissipation lengths exceed predicted cooperation lengths by one order of magnitude. Recent developments based on a Glarum Levy defect interpretation of the dynamic transition suggest that a divergence of ξ_α is unlikely[36] and thus the divergence of $X_d(T)$ towards the calorimetric glass transition cannot be explained solely based on heterogeneous growth of CRRs. The divergent domain size $X_d(T)$ likely reflects long-range relaxation modes, e.g., the normal mode (overall chain dynamics)[26] or Fischer modes, that couple with the α-relaxation mode of the FFM signal.[39] At higher temperatures, the α and normal modes can be described by the same apparent activation energy; however, in the vicinity of T_g, the α mode can decouple from the normal mode. Below this point, the length scale for the α relaxation remains strongly temperature dependent, whereas that for the normal mode relaxation is relatively invariant with temperature.[26] Considering we do not observe any change in the process activation energy in the divergent region and that $X_d(T)$ does not saturate to a temperature-independent value, it is unlikely that the FFM probe is sensitive to the normal mode. Alternatively, the departure of the structural and α-relaxation times close to T_g could lead to a nonergodic behavior with coupling of ultraslow, long-range, correlated density fluctuations with the α relaxation.[39,44,45] Based on light-scattering studies by Fischer *et al.*, long-range density fluctuations are expected in the vicinity of T_g. These *far-field* effects involve slow relaxations, $\tau_{\text{slow}} = 10^7 \tau_\alpha$, with a cooperation length up to two orders of magnitude larger than the characteristic length of the α relaxation discussed above.[45,46] Although our experiment, based on its small contact size and experimentally applicable velocities, should be insensitive to such long-range density fluctuations, the ultraslow process can couple to the α relaxation, leading to apparent nonergodic time-averaged correlations occurring on the time scale of the α relaxation.[45]

Finally, it should be noted that in many experiments, the structural relaxation time is comparable to the α-relaxation time τ_α for $1 \text{ ms} < \tau_\alpha < 100$ ms.[47] This time regime is applicable to most of the data discussed in Fig. 4 except for the two divergent points at $T = 377$ and 380 K, with relaxation times of 3700 and 430 ms, respectively. The potential departure of the structural and α-relaxation times in this region questions the applicability of Eq. (1) very close to T_g, and the impact on the length scale is part of future investigations.

IV. CONCLUSION

Nanoscale friction involving polymer melts near the glass transition showed a dissipation phenomenon that provides insight to the underlying molecular relaxation processes. Our study benefited from the real-space molecular sensitivity of a nanoscopic probe and from spectroscopic time-temperature data. Frictional dissipation in the polystyrene melt could be directly linked to the α-relaxation process and thus *elastomeric friction* is described in terms of a rheological model, in which energy is dissipated through activated molecular relaxations in the *soft* material.

The freezing of the α relaxation through a crossover-type region $(T_g < T < T_2)$ was reflected in both the friction coefficient and the friction-velocity peak intensities, which led to a discussion of dissipation in light of the cooperative motion expected for a dynamic glass transition. The characteristic length of the dissipation process grew from the segmental scale to 2.1 nm, following a power-law behavior that appears consistent with predictions for cooperative motion during the α relaxation. However, in the vicinity of T_g, dissipation lengths of several tens of nanometers deviate from the above power-law behavior. The large dissipation lengths suggest that long-range processes may couple with the α relaxation with an apparent nonergodic time-averaged behavior. The resulting length scale of dissipation exhibited a diverging behavior towards T_g, not unlike that expected for the viscosity.

The large size of the dissipation lengths near the glass transition warrants attention. Compared to structures in modern device technologies, e.g., ultrathin films and nanocomposites involving sub-100-nanometer dimensions, one can expect a competition between material and device length scales. Consequently, material properties in dimensionally constrained systems are likely to be modified from their original bulk values as found, for instance, in SM-FM analysis of ultrathin PS films[48] and Brillouin light scattering.[49] The impact of dimensional constraints on the dissipation behavior will provide valuable insight to the development of technologically relevant polymer materials for photonics,[10] electronics,[12] and nanoelectromechanical systems (NEMS).

ACKNOWLEDGMENTS

We gratefully acknowledge E. Donth from Universität Halle, Germany for providing the V_α data used in Fig. 5 and Clayton Henderson from Hitachi Global Storage for fruitful discussions pertaining to relaxation length scales. This work was supported in part by IBM, the University of Washington Center for Nanotechnology, the Petroleum Research Fund administered by the American Chemical Society, and the Royalty Research Fund of the University of Washington.

[1] V. N. Pokrovskii, *Mesoscopic Theory of Polymer Dynamics* (Kluwer Academic, Dordrecht, 2000).
[2] K. A. Grosch, Proc. R. Soc. London, Ser. A **274**, 21 (1963).
[3] K. C. Ludema and D. Tabor, Wear **9**, 329 (1966).
[4] M. L. Williams, R. F. Landel, and J. D. Ferry, J. Am. Chem. Soc. **77**, 3701 (1955).
[5] A. Schallamach, Wear **6**, 375 (1953).
[6] T. Kontorova and Y. I. Frenkel, Zh. Eksp. Teor. Fiz. **8**, 1340 (1938).
[7] H. Eyring, J. Chem. Phys. **4**, 283 (1936).
[8] Y. B. Chernyak and A. I. Leonov, Wear **108**, 105 (1986).
[9] O. Ronsin and K. L. Coeyrehourcq, Proc. R. Soc. London, Ser. A **457**, 1277 (2001); K. Vorvolakos and M. K. Chaudhury, Langmuir **19**, 6778 (2003).
[10] J. Luo, M. Haller, H. Ma *et al.*, J. Phys. Chem. B **108**, 8524 (2004).
[11] T. Gray, R. M. Overney, M. Haller, J. Luo, and A. K.-Y. Jen, Appl. Phys. Lett. **86**, 211908 (2005).
[12] A. P. Kulkarni and S. A. Jenekhe, Macromolecules **36**, 5285 (2003).
[13] P. Vettiger, G. Cross, M. Despont *et al.*, IEEE Trans. Nanotechnol. **1**, 39 (2002).
[14] R. Overney and E. Meyer, MRS Bull. **18**, 26 (1993).
[15] R. W. Carpick and M. Salmeron, Chem. Rev. (Washington, D.C.) **97**, 1163 (1997).
[16] R. M. Overney, C. Buenviaje, R. Luginbuehl, and F. Dinelli, J. Therm Anal. Calorim. **59**, 205 (2000).
[17] C. K. Buenviaje, S. R. Ge, M. H. Rafailovich, and R. M. Overney, Mater. Res. Soc. Symp. Proc. **552**, 187 (1998).
[18] R. H. Schmidt, G. Haugstad, and W. L. Gladfelter, Langmuir **19**, 10390 (2003); B. Gotsmann and U. Dürig, *ibid.* **20**, 1495 (2004).
[19] S. Sills and R. M. Overney, Phys. Rev. Lett. **91**, 095501 (2003).
[20] D. Michel, S. Kopp-Marsaudon, and J. P. Aime, Tribol. Lett. **4**, 75 (1998).
[21] K. G. McLaren and D. Tabor, Nature (London) **197**, 856 (1963); T. Aoiki, H. Uehara, T. Yamanobe, and T. Komoto, Langmuir **17**, 2153 (2001).
[22] D. Schrader, in *Polymer Handbook*, edited by J. Brandrup, E. H. Immergut, and E. A. Grulke (Wiley, New York, 1999), p. V.
[23] J. D. Ferry, *Viscoelastic Properties of Polymers*, 3rd ed. (Wiley, New York, 1980).
[24] G. D. Patterson, C. P. Lindsey, and J. R. Stevens, J. Chem. Phys. **70**, 643 (1979); R. F. Boyer and S. G. Turley, in *Molecular Basis of Transitions and Relaxations*, edited by D. J. Meier (Gordon and Breach, New York, 1978), p. 335.
[25] J. A. Hammerschmidt, W. L. Gladfelter, and G. Haugstad, Macromolecules **32**, 3360 (1999).
[26] A. Schönhals and E. Schlosser, Phys. Scr. **T49**, 233 (1993).
[27] M. Biener, H. Huth, and K. Schroeter, J. Non-Cryst. Solids **279**, 126 (2001).
[28] H. Sillescu, J. Non-Cryst. Solids **243**, 81 (1999).
[29] P. G. Debenedetti and F. H. Stillinger, Nature (London) **410**, 259 (2001); V. P. Biju, J. Y. Ye, and M. Ishikawa, J. Phys. Chem. B **107**, 10729 (2003).
[30] T. Kanaya, T. Kawaguchi, and K. Kaji, J. Chem. Phys. **104**, 3841 (1995).
[31] C. M. Roland and R. Casalini, J. Chem. Phys. **119**, 1838 (2003).
[32] P. Hedvig, *Dielectric Spectroscopy of Polymers* (Wiley, New York, 1977).
[33] E. Donth, J. Polym. Sci., Part B: Polym. Phys. **34**, 2881 (1996).
[34] R. Richert, J. Phys.: Condens. Matter **14**, R703 (2002).
[35] H. Sillescu, R. Bohmer, G. Diezemann, and G. Hinze, J. Non-Cryst. Solids **307**, 16 (2002); M. D. Ediger, Annu. Rev. Phys. Chem. **51**, 99 (2000).
[36] E. Donth, J. Non-Cryst. Solids **307–310**, 364 (2002).
[37] C. Y. Wang and M. D. Ediger, J. Phys. Chem. B **104**, 1724 (2000).
[38] U. Tracht, M. Wilhelm, A. Heuer, H. Feng, K. Schmidt-Rohr, and H. W. Spiess, Phys. Rev. Lett. **81**, 2727 (1998).
[39] A. S. Bakai and E. W. Fischer, J. Chem. Phys. **120**, 5235 (2003).
[40] E. Donth, Phys. Scr. **T49**, 223 (1993).
[41] F. Garwe, M. Beiner, E. Hempel, J. Schawe, K. Schröter, A. Schönhals, and E. Donth, J. Non-Cryst. Solids **172–174**, 191 (1994).
[42] C. Bennemann, C. Donati, J. Baschnagel, and S. Glotzer, Nature (London) **399**, 246 (1999).
[43] H. Huth, Ph.D. thesis, Universität Halle, 2001.
[44] E. W. Fischer, A. Bakai, A. Patkowski, W. W. Steffen, and L. Reinhardt, J. Non-Cryst. Solids **307–310**, 584 (2002).
[45] A. Patkowski, H. Glaser, T. Kanaya, and E. W. Fischer, Phys. Rev. E **64**, 031503 (2001).
[46] T. Kanaya, A. Patkowski, E. W. Fischer, J. Seils, H. Glaeser, and K. Kaji, Macromolecules **28**, 7831 (1995).
[47] H. Sillescu, J. Phys.: Condens. Matter **11**, A271 (1999).
[48] S. E. Sills, R. M. Overney, W. Chau, V. Y. Lee, R. D. Miller, and J. Frommer, J. Chem. Phys. **120**, 5334 (2004).
[49] J. A. Forrest, K. Dalnoki-Veress, and J. R. Dutcher, Phys. Rev. E **58**, 6109 (1998).

The Journal of Chemical Physics is copyrighted by the American Institute of Physics (AIP). Redistribution of journal material is subject to the AIP online journal license and/or AIP copyright. For more information, see http://ojps.aip.org/jcpo/jcpcr/jsp